Physics Letters B 788 (2019) 446–452

Contents lists available at ScienceDirect

Physics Letters B

www.elsevier.com/locate/physletb

Non-commutative inspired black holes in Euler–Heisenberg non-linear electrodynamics

Marco Maceda *, Alfredo Macías

Departamento de Física, Universidad Autónoma Metropolitana-Iztapalapa. A.P. 55-534, C.P. 09340 Mexico City, México

ARTICLE INFO

Article history:
Received 18 October 2018
Received in revised form 14 November 2018
Accepted 27 November 2018
Available online 29 November 2018
Editor: M. Cvetič

Keywords:
Euler–Heisenberg non-linear electrodynamics
Non-commutative smeared distributions
Shadow of a black hole
Energy conditions

ABSTRACT

We find non-commutative inspired electrically and magnetically charged black hole solutions in Euler–Heisenberg non-linear electrodynamics. We analyse the weak energy condition and show that it is satisfied in opposition to the commutative case. We also obtain the shadow associated with these metrics that may be susceptible to observation.

1. Introduction

A quantum theory of gravity is a central challenge nowadays. A certain number of proposals exist to analyse quantum effects in gravitational fields (loop quantum gravity, string theory, non-commutative geometry, matrix geometry). All of them cover several aspects at different levels and complement each other; this interplay provides us with useful insights into the whole picture.

In some of these approaches, the structure of space–time is assumed to lose its continuum character. Such discretisation implies generalised uncertainty principles that are natural consequences of a quantum theory of gravity where we have a set of coordinate and momentum operators with a discrete spectrum. In the general case, the commutation relations among the coordinates and momentum operators imply the existence of a minimal length [1]. This length serves as a natural cutoff that removes divergences from the theory.

If we want to implement commutation relations among spatial coordinates only, we may use a star product that is a consequence of the commutation relations and replaces the standard point-wise multiplication of functions. The use of star products to encode non-commutative effects generally leads to perturbative calculations. More recently, an approach [2] based on non-commutative coherent states allows the analysis of non-perturbative effects. This analysis, initially motivated by calculations in non-commutative quantum field theory [3,4], showed that a non-commutative Gaussian smeared distribution is the appropriate replacement for the point-like behaviour of particles usually present in a commutative setup.

In General Relativity this idea allows the construction of non-commutative inspired black holes. These objects have the standard properties associated with black holes, but they are regular at the source of the gravitational field; they possess an inner de Sitter core that cures the curvature singularity. Nowadays, we know a rich variety of non-commutative inspired black hole solutions. They include the non-commutative inspired Schwarzschild and Reissner–Nordström (RN) metrics [5,6]. More recently, the Kerr and Kerr–Newman solutions have been obtained using a modified Janis–Newman algorithm specially tailored for the non-commutative framework [7].

On the other hand, non-linear electrodynamics extends our knowledge of the electromagnetic field and its physical effects. It is a natural consequence when looking for a solution to the self-energy problem of a point charged particle. The Born–Infeld (BI) electrodynamics [8] is the first example of this. It is also a natural outcome when taking into account loop corrections in QED for instance, where the Euler–Heisenberg (EH) electrodynamics [9] be-

* Corresponding author.
E-mail addresses: mmac@xanum.uam.mx (M. Maceda), amac@xanum.uam.mx (A. Macías).

https://doi.org/10.1016/j.physletb.2018.11.048

comes relevant. Both electrodynamics describe phenomena outside the realm of standard Maxwell's equations. The recent observations of Sgr A* indicate that a massive black hole lies at the centre of the Milky Way, and this feature is believed to be present in the majority of the active galactic nuclei known to date. We expect then modifications on the behaviour of particles at the vicinity of these supermassive black holes; in this regard, the orbital motion of photons is a useful tool to determine the shadow of the black hole [10–14]. Furthermore, since the medium around the black hole involves matter interacting not only gravitationally but also electromagnetically, the existence of jets of charged particles is a common phenomenon, we also expect effects due to non-linear electrodynamics to be present as well. Previous results in this direction may be found in the literature [15,16].

To gain more insight into the aspects mentioned previously, we consider in this work non-commutative inspired charged black holes in EH electrodynamics. We include non-commutative effects by using smeared distributions of mass and charge, and we choose to work with EH non-linear electrodynamics because it contains all the characteristic features present in more complex non-linear electrodynamics, such as BI electrodynamics. Furthermore, from a practical point of view, it is more amenable to give us analytic results. The use of more advanced interferometers opens the possibility to observe a black hole directly in the future and to test models and theories analysing the quantum structure of spacetime at microscopic length scales.

We organise this Letter as follows: in Sec. 2 we construct the corresponding non-commutative inspired black holes, and we analyse the weak energy condition in Sec. 3 and we investigate how the non-commutative parameter affects the shadow of the non-commutative inspired black holes in Sec. 4. We end with some remarks and perspectives in the Conclusions.

2. Non-commutative inspired black holes with electric and magnetic charge from Euler–Heisenberg electrodynamics

Non-commutative inspired models are solutions of the modified gravitational field equations [3,4,2,5,6,17–20]

$$R_{\mu\nu} - \frac{1}{2} g_{\mu\nu} R = 8\pi [\mathfrak{T}_{\mu\nu} + T^{e.m.}_{\mu\nu}], \tag{1}$$

where

$$\mathfrak{T}^{\mu}{}_{\nu} := diag(h_1, h_1, h_3, h_3), \tag{2}$$

is a non-commutative energy–matter tensor and $T^{e.m.}_{\mu\nu}$ is the standard electromagnetic tensor. The function h_1 in $\mathfrak{T}^{\mu}{}_{\nu}$ is given by

$$h_1 := -\rho_m(r) = -\frac{\mathcal{M}}{(4\pi\theta)^{3/2}} e^{-r^2/4\theta}, \tag{3}$$

where θ is the non-commutative parameter and $h_3 := (r^2 h_1)_{,r}/2r$ is such that the conservation law $\nabla_\mu \mathfrak{T}^{\mu\nu} = 0$ holds; the normalisation of $\rho_m(r)$

$$\int d^d x \, \rho_m(r) = \mathcal{M}, \tag{4}$$

gives the mass of a classical point-like source of the gravitational field. In the commutative limit $\theta \to 0$, the smeared distribution $\rho_m(r)$ becomes a Dirac delta function.

The motivation and justification of these smeared distributions to encode non-commutative effects were first discussed in the context of quantum field theory and afterwards extended to the gravitational arena in the static and rotating scenarios [3–5,2,7,20]. In the following sections, we solve the non-commutative field equations assuming a static spherically symmetric spacetime

$$ds^2 = -\left[1 - \frac{2m(r)}{r}\right] dt^2 + \left[1 - \frac{2m(r)}{r}\right]^{-1} dr^2 + r^2 d\Omega, \tag{5}$$

where $d\Omega := d\vartheta^2 + \sin^2\vartheta d\phi^2$, coupled to the EH Lagrangian

$$\mathcal{L}_{EH} = -x + \frac{A}{2} x^2 + \frac{B}{2} y^2. \tag{6}$$

Here $x := \frac{1}{4} F_{\mu\nu} F^{\mu\nu}$, $y := \frac{1}{4} F_{\mu\nu} \star F^{\mu\nu}$ are the relativistic invariants of the electromagnetic field, and $F_{\mu\nu}$ is the electromagnetic tensor; the relation between the above coefficients is $B = 7A/4$. Using a Legendre transformation, a dual description of the EH Lagrangian is

$$\hat{\mathcal{L}}_{EH} = s - \frac{A}{2} s^2 - \frac{B}{2} t^2, \tag{7}$$

up to terms linear on A and B. Here $s := -\frac{1}{4} P_{\mu\nu} P^{\mu\nu}$, $t := -\frac{1}{4} P_{\mu\nu} \star P^{\mu\nu}$ are the dual relativistic invariants of the electromagnetic field, and $P_{\mu\nu} := -(\mathcal{L}_x F_{\mu\nu} + \mathcal{L}_y \star F_{\mu\nu})$ are the Plebanski variables [21–24]. The standard Lagrangian uses the electric field E and the magnetic induction B while the dual description uses the displacement field D and the magnetic field H. In the purely electric charged case the invariants y and t vanish, meanwhile in the purely magnetic case the invariants x and s vanish. This duality transformation also holds in the non-commutative case because the structure of the EH Lagrangian is not modified.

2.1. Non-commutative inspired electric solution

For the electrically charged case we solve the non-commutative conservation laws

$$\nabla_\mu P^{\mu\nu} = 4\pi J^\mu, \tag{8}$$

where

$$J^\mu = Q_e \left[\frac{e^{-r^2/4\theta}}{(4\pi\theta)^{3/2}}, 0, 0, 0 \right], \tag{9}$$

is a source for the electric field having a non-commutative origin. This source basically replaces the point-like behaviour of the delta function by an electrically charged smeared distribution depending on the non-commutative parameter. The solution to Eq. (8) is then given by the non-commutative inspired Plebanski variables

$$P_{\mu\nu} = \frac{2}{\sqrt{\pi}} \frac{Q_e}{r^2} \gamma\left(\frac{3}{2}, \frac{r^2}{4\theta}\right) \delta^0_{[\mu} \delta^1_{\nu]}, \tag{10}$$

where $\gamma(a, z)$ is the lower incomplete gamma function [25]. The relevant field equation is now

$$\frac{m_{,r}}{r^2} = \frac{1}{2} P_{01}^2 - \frac{1}{8} A P_{01}^2 + \frac{\mathcal{M}}{2\sqrt{\pi}\theta^{3/2}} e^{-r^2/4\theta}. \tag{11}$$

The non-commutative inspired electrically charged black hole in this case is then

$$ds^2 = -\left[1 - \frac{4\mathcal{M}}{r\sqrt{\pi}} \gamma\left(\frac{3}{2}, \frac{r^2}{4\theta}\right) - \frac{4}{\pi} \frac{Q_e^2}{r} \times \int_0^r \frac{ds}{s^2} \gamma^2\left(\frac{3}{2}, \frac{s^2}{4\theta}\right)\right.$$

$$+\frac{4A}{\pi^2}\frac{Q_e^4}{r}\int_0^r \frac{ds}{s^6}\gamma^4\left(\frac{3}{2},\frac{s^2}{4\theta}\right)\Bigg]dt^2$$
$$+\Bigg[1-\frac{4\mathcal{M}}{r\sqrt{\pi}}\gamma\left(\frac{3}{2},\frac{r^2}{4\theta}\right)-\frac{4}{\pi}\frac{Q_e^2}{r}$$
$$\times\int_0^r\frac{ds}{s^2}\gamma^2\left(\frac{3}{2},\frac{s^2}{4\theta}\right)$$
$$+\frac{4A}{\pi^2}\frac{Q_e^4}{r}\int_0^r \frac{ds}{s^6}\gamma^4\left(\frac{3}{2},\frac{s^2}{4\theta}\right)\Bigg]^{-1}dr^2$$
$$+r^2d\Omega, \tag{12}$$

where $\mathcal{M}$ is the "bare" mass. Using instead the ADM mass [6]

$$M := \oint_\Sigma d\sigma^\mu (T^0_\mu|_{matt} + T^0_\mu|_{el}), \tag{13}$$

we have

$$ds^2 = -f(r)dt^2 + f(r)^{-1}dr^2 + r^2 d\Omega, \tag{14}$$

with

$$f(r) =$$
$$1-\frac{4M}{r\sqrt{\pi}}\gamma\left(\frac{3}{2},\frac{r^2}{4\theta}\right)+\frac{1}{\pi}\frac{Q_e^2}{r^2}\gamma^2\left(\frac{1}{2},\frac{r^2}{4\theta}\right)$$
$$+\frac{1}{\pi}\frac{Q_e^2}{r^2}\Bigg[\sqrt{\frac{2}{\theta}}r\gamma\left(\frac{3}{2},\frac{r^2}{4\theta}\right)$$
$$-\frac{r}{\sqrt{2\theta}}\gamma\left(\frac{1}{2},\frac{r^2}{2\theta}\right)\Bigg]-\frac{4A}{\pi^2}\frac{Q_e^4}{r}$$
$$\times\int_r^\infty\frac{ds}{s^6}\gamma^4\left(\frac{3}{2},\frac{s^2}{4\theta}\right)+\frac{A}{8\pi^2}\frac{Q_e^4}{r}$$
$$\times\left[1-\frac{2}{\sqrt{\pi}}\gamma\left(\frac{3}{2},\frac{r^2}{4\theta}\right)\right]\frac{\alpha}{\theta^{5/2}}, \tag{15}$$

where $\alpha := \int_0^\infty ds\, s^{-6}\gamma^4\left(\frac{3}{2},s^2\right) = 0.02757$ and we have used the identity [25] $\gamma(\frac{a}{2}+1,z^2)=\frac{a}{2}\gamma(\frac{a}{2},z^2)-z^a e^{-z^2}$ to obtain the second equality. Fig. 1 shows a generic plot of the function $f(r)$; the non-commutative solution is regular at the origin and there is a value θ_{crit} above which the non-commutative solution becomes an everywhere regular spacetime with no horizons. In the commutative limit $\theta \to 0$, we recover the commutative EEH metric [26]

$$ds^2 =$$
$$-\left(1-\frac{2M}{r}+\frac{Q_e^2}{r^2}-\frac{A}{20}\frac{Q_e^4}{r^6}\right)dt^2$$
$$+\left(1-\frac{2M}{r}+\frac{Q_e^2}{r^2}-\frac{A}{20}\frac{Q_e^4}{r^6}\right)^{-1}dr^2$$
$$+r^2d\Omega. \tag{16}$$

2.2. Non-commutative inspired magnetic solution

The magnetic charged solution is defined by the non-commutative inspired electromagnetic tensor

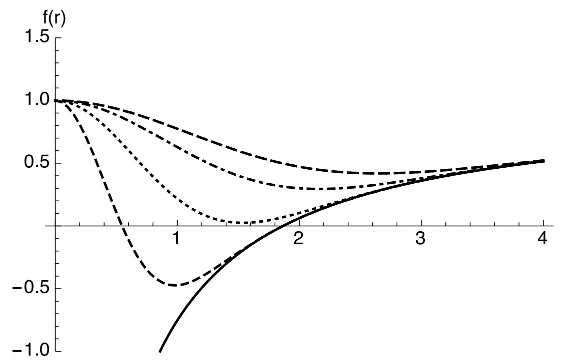

Fig. 1. Plot of the non-commutative function $f(r)$ for values of $\theta = 0.1, 0.25, 0.5$ and 0.7 (dashed lines from bottom to top) with $M = 1$, $Q_e = 0.5$, $A = 1$. The solid line corresponds to the commutative EEH spacetime; there is value θ_{crit} above which the non-commutative solution becomes an everywhere regular spacetime without horizons.

$$F_{\mu\nu} = -\frac{2}{\sqrt{\pi}}Q_m\gamma\left(\frac{3}{2},\frac{r^2}{4\theta}\right)\sin\vartheta\,\delta^2_{[\mu}\delta^3_{\nu]}, \tag{17}$$

and the field equation to be considered now is then

$$\frac{m_{,r}}{r^2} = -s + \frac{3A}{2}s^2 + \frac{\mathcal{M}}{2\sqrt{\pi}\theta^{3/2}}e^{-r^2/4\theta}, \tag{18}$$

where s is defined as

$$s := -\frac{1}{2}\frac{Q_m^2}{r^4}\left(-1+\frac{A}{2}\frac{Q_m^2}{r^4}\right)^2. \tag{19}$$

Therefore, the non-commutative inspired magnetically charged black hole is

$$ds^2 =$$
$$-\Bigg[1-\frac{4\mathcal{M}}{r\sqrt{\pi}}\gamma\left(\frac{3}{2},\frac{r^2}{4\theta}\right)-\frac{4}{\pi}\frac{Q_m^2}{r}$$
$$\times\int_0^r\frac{ds}{s^2}\gamma^2\left(\frac{3}{2},\frac{s^2}{4\theta}\right)$$
$$+\frac{4A}{\pi^2}\frac{Q_m^4}{r}\int_0^r \frac{ds}{s^6}\gamma^4\left(\frac{3}{2},\frac{s^2}{4\theta}\right)\Bigg]dt^2$$
$$+\Bigg[1-\frac{4\mathcal{M}}{r\sqrt{\pi}}\gamma\left(\frac{3}{2},\frac{r^2}{4\theta}\right)-\frac{4}{\pi}\frac{Q_m^2}{r}$$
$$\times\int_0^r\frac{ds}{s^2}\gamma^2\left(\frac{3}{2},\frac{s^2}{4\theta}\right)$$
$$+\frac{4A}{\pi^2}\frac{Q_m^4}{r}\int_0^r \frac{ds}{s^6}\gamma^4\left(\frac{3}{2},\frac{s^2}{4\theta}\right)\Bigg]^{-1}dr^2$$
$$+r^2d\Omega. \tag{20}$$

As previously, this metric can be rewritten in terms of the ADM mass M as defined in Eq. (13); we obtain then a metric similar to Eq. (14) where $f(r)$ is exactly the same function as in Eq. (15) but with Q_e replaced by Q_m. The non-commutative charged EEH metrics are related by the same functional expression as it happens in the classical case.

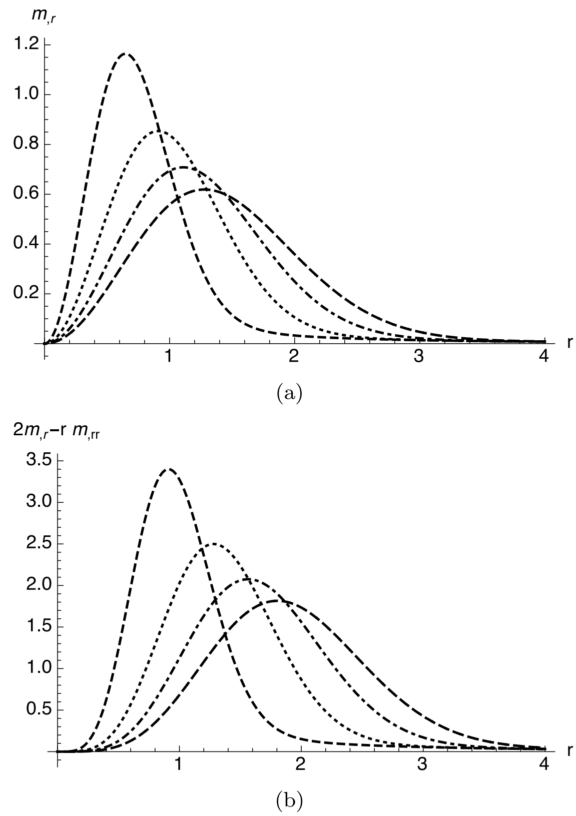

Fig. 2. Plots of the first and second energy conditions for values of $\theta = 0.1, 0.2, 0.3$ and 0.4 (dashed lines from top to bottom) with $M = 1$, $Q_e = 0.5$, $A = 0.1$ (non-commutative EEH black hole with one horizon).

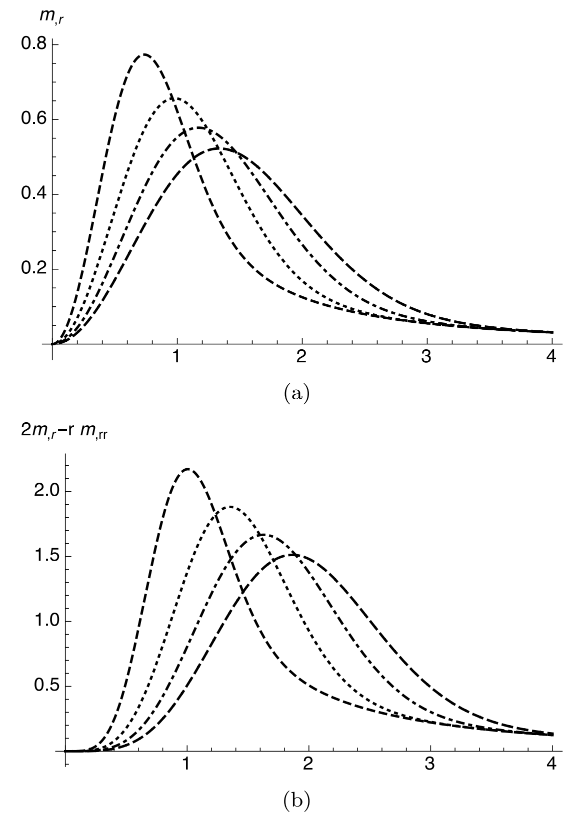

Fig. 3. Plots of the first and second energy conditions for values of $\theta = 0.1, 0.2, 0.3$ and 0.4 (dashed lines from top to bottom) with $M = 1.02$, $Q_e = 1$, $A = 0.3$ (non-commutative EEH black hole with three horizons).

3. Weak energy condition

We recall first that the strong, dominant and weak energy conditions are

- Strong Energy Condition (SEC): $T_{\mu\nu}t^\mu t^\nu \geq \frac{1}{2}T^\mu{}_\mu t^\nu t_\nu$ for any timelike vector t^μ,
- Dominant Energy Condition (DEC): $T_{\mu\nu}t^\mu t^\nu \geq 0$ and $T^{\mu\nu}t_\nu$ must be timelike or null for any timelike vector t^μ,
- Weak Energy Condition (WEC): $T_{\mu\nu}t^\mu t^\nu \geq 0$, for any timelike vector t^μ.

The DEC is often recast as $T^{00} \geq |T^{ij}|$ with $i, j = 1, 2, 3$; it implies the WEC, which is often expressed as the conditions

$$m_{,r} \geq 0, \qquad 2m_{,r} \geq r m_{,rr}. \tag{21}$$

We consider now the WEC in our model and without loss of generality, we focus on the electric solution. Due to the presence of the lower incomplete gamma function, an explicit expression for the above inequalities is rather cumbersome and not illuminating. For this reason, we show instead in Fig. 2 the generic plots for a solution with a single horizon and in Fig. 3 the plots for a solution with three horizons. We remark that in these plots, the two conditions associated to the WEC are satisfied everywhere for the values chosen for the parameters.

The electric charged EEH solution is regular at the source. It is a known fact that regular solutions violate the SEC, meanwhile the WEC may or may not be satisfied. Let us focus on the behaviour near the origin; a straightforward calculation shows that for $r \to 0$, we have

$$\begin{aligned} m_{,r} &= \\ &\frac{\left(A\alpha Q_e^4 + 16\pi^2\theta^{5/2}M - 4\sqrt{2}\pi^{3/2}\theta^2 Q_e^2\right)}{32\pi^{5/2}\theta^4}r^2 \\ &+ O(r^4), \\ 2m_{,r} - rm_{,rr} &= \\ &\frac{\left(9A\alpha Q_e^4 + 144\pi^2\theta^{5/2}M - 4(4+9\sqrt{2})\pi^{3/2}\theta^2 Q_e^2\right)}{576\pi^{5/2}\theta^5}r^4 \\ &+ O(r^5). \end{aligned} \tag{22}$$

From these expressions we see then that the non-commutative EEH solution Eq. (15), and also its magnetic counterpart, *does* satisfy the WEC in a region near the origin depending on the values of the parameters M, Q_e, A and θ; a rough condition for this behaviour is $\sqrt{\theta}M \geq 0.263 Q_e^2$. This result is in contrast with the commutative EEH solution where the WEC is always violated near the origin. It is also a straightforward calculation to show that the EEH non-commutative inspired black hole satisfies the null energy condition.

4. Shadow of the non-commutative Einstein–Euler–Heisenberg black hole

As astrophysical objects, black holes provide useful insights in the structure of space–time. We now address the formation of a shadow for the non-commutative inspired black holes in EH electrodynamics. From the metric we obtain the Lagrangian

$$2\mathcal{L} = -f(r)\dot{t}^2 + f(r)^{-1}\dot{r}^2 + r^2\dot{\theta}^2 + r^2\sin^2\theta\dot{\phi}^2, \tag{23}$$

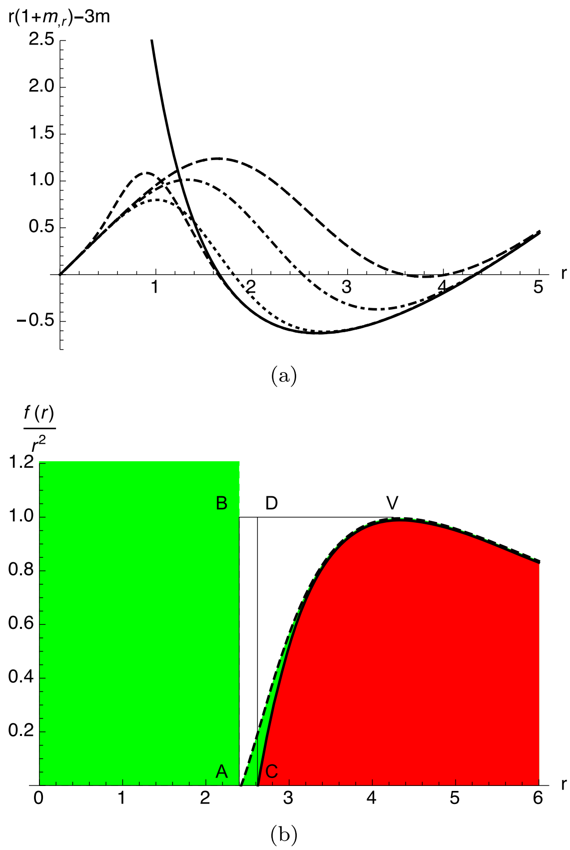

Fig. 4. (a) is a plot of the condition determining the existence of circular photon radial orbits; the solid line correspond to the commutative case with $M = 2$, $Q = 1.9$ and $A = 0$ (RN) and the dashed lines (from bottom to top) correspond to the values $\theta = 0.1, 0.25, 0.5$ and 0.75. (b) shows the forbidden regions for rays for $\theta = 0$ (red region) and $\theta = 0.4$ (green+red region). The domains of recapture of rays are the curvilinear triangles CDV and ABV for the commutative and non-commutative cases respectively (the vertical axis has been scaled for illustrative purposes).

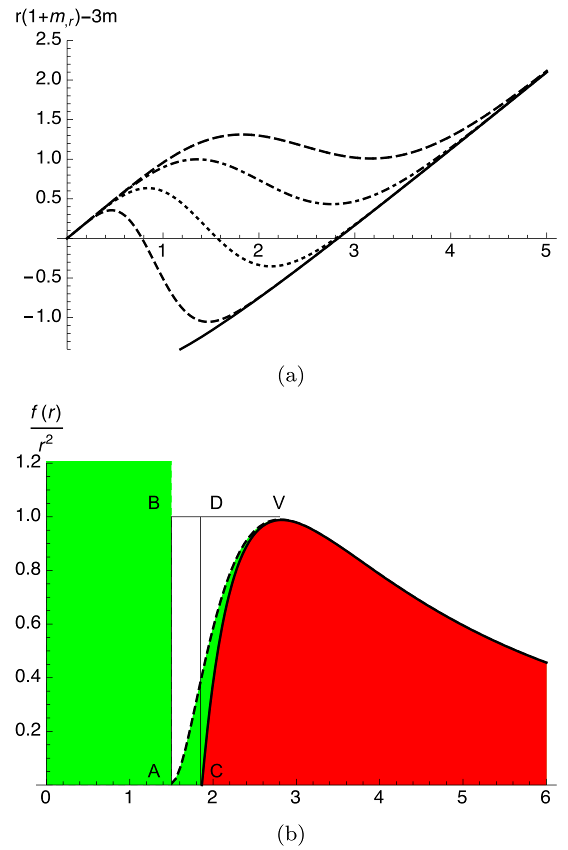

Fig. 5. (a) is a plot of the condition determining the existence of circular photon radial orbits; the solid line correspond to the commutative case with $M = 1$, $Q = 0.5$ and $A = 1$ (EEH) and the dashed lines (from bottom to top) correspond to the values $\theta = 0.1, 0.25, 0.5$ and 0.75. (b) shows the forbidden regions for rays for $\theta = 0$ (red region) and $\theta = 0.237$ (green+red region). The domains of recapture of rays are the curvilinear triangles CDV and ABV for the commutative and non-commutative cases respectively (the vertical axis has been scaled for illustrative purposes).

where a dot denotes derivative with respect to the affine parameter. This Lagrangian provides the starting point to the analysis of orbital motion of test particles and its value determines the orbits under study; for massive and null orbits we have $2\mathcal{L} = +1, 0$ respectively.

Due to the independence of the metric on the time and azimuthal variable, in general there are two conserved quantities of motion

$$p_t = -f(r)\dot{t} = -E,$$
$$p_\phi = r^2 \sin^2\theta \dot{\phi} = L, \tag{24}$$

related to the energy and angular momentum of the test particle. In the following we consider the existence of a shadow and therefore restrict ourselves to the case of photon orbits ($\mathcal{L} = 0$). Solving for $\dot{t}$ and $\dot{\phi}$ from Eqs. (24) and substituting into the Lagrangian, we obtain the equation

$$\dot{r}^2 + f r^2 \dot{\theta}^2 + \frac{L^2 f - E^2 r^2 \sin^2\theta}{r^2 \sin^2\theta} = 0. \tag{25}$$

Since we are dealing with spherical symmetric solutions to the field equations, the associated shadow of the non-commutative EEH black hole will be circularly symmetric. In consequence, we can fix $\theta = \pi/2, \dot{\theta} = 0$, knowing that the results are then valid in general. Therefore, with this choice and from the previous equation we identify the effective potential

$$V_{eff}(r) = L^2 \frac{f}{r^2} - E^2. \tag{26}$$

Circular photon orbits at a radius r_{ph} are then determined by the conditions $V_{eff}(r_{ph}) = 0 = V_{eff,r}(r_{ph})$, or equivalently

$$b^2 = \frac{r_{ph}^2}{f(r_{ph})}, \qquad r_{ph} f_{,r}(r_{ph}) - 2f(r_{ph}) = 0, \tag{27}$$

where $b := L/E$ is the impact parameter. In terms of the function $m(r)$, the last equation becomes

$$r_{ph}[m_{,r}(r_{ph}) + 1] - 3m(r_{ph}) = 0. \tag{28}$$

In Figs. 4(a) and 5(a), we plot the left hand side of Eq. (28) with $M = 2$, $Q = 1.9$, $A = 0$ (RN) and $M = 1$, $Q = 0.5$, $A = 1$ (EH) respectively for various values of θ. From these plots we see that there is a precise value above which the left-hand side of Eq. (28) does not vanish; the absence of roots for this equation is an indication that the non-commutative black hole solution becomes a spacetime that is regular everywhere and has no horizons. In Figs. 4(b) and 5(b) we show the allowed regions for the escape of photons along the lines of [27]. In the non-commutative case, points inside the curvilinear triangles ABV (CDV in the commutative case) correspond to rays with an apse; these rays cannot escape and fall into the black hole. On the contrary, all rays to the

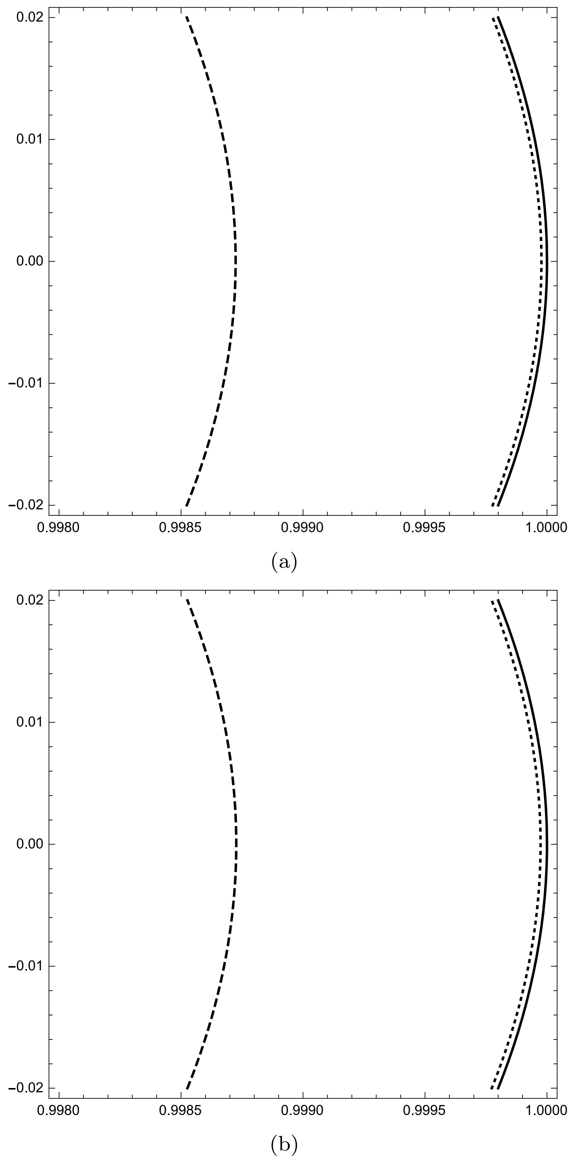

Fig. 6. Detail of the shadow of the non-commutative inspired EEH black hole with $M = 2$, $Q = 1.9$. (a) shows the case for $A = 0$ (RN) with $\theta = 0, 0.4, 0.6$ (from outer to inner). (b) shows the case for $A = 1$ (EEH) with $\theta = 0, 0.4, 0.6$ (from outer to inner). In each case, for convenience, the radius of the shadow is given by the ratio b^{nc}/b^{comm} between the non-commutative impact parameter and the commutative value.

right of the point V escape to infinity. The value of r at the point V gives then the size of the shadow of the non-commutative black hole.

The non-commutative correction to the commutative value r_{ph} seems to be small. Further analysis shows that the value of r_{ph} for the non-commutative black hole, either RN or EEH, is less than the commutative one; the difference in these values is slightly more visible when the EH electrodynamics is turned on. Regarding the impact parameter b, we can use Eq. (27) to evaluate it in the non-commutative case. It is seen that we have now a smaller shadow associated with the non-commutative inspired EH black holes. As mentioned before, the correction is small: in Fig. 6(a), the impact parameter has the values $8.3523, 8.3521$ and 8.3417 for $\theta = 0, 0.4, 0.6$ (from outer to inner) when $A = 0$ (RN); in Fig. 6(b), it has the values $8.3538, 8.3536$ and 8.3432 for $\theta = 0, 0.2, 0.237$ (from outer to inner) when $A = 1$ (EEH).

5. Conclusions

We have constructed the non-commutative inspired static electric and magnetic charged black holes coupled to Euler–Heisenberg non-linear electrodynamics. For that purpose, we considered non-commutative smeared distributions that replace the point-like behaviour of sources.

The non-commutative generalisation of the electrical charged EEH spacetime is quite straightforward using the modified field equations. The appearance of lower incomplete gamma functions in the metric is a characteristic feature of these kinds of solutions, providing the mechanism for a non-singular behaviour at the location of the source. The non-commutative inspired magnetic charged EEH spacetime has the same functional form as the non-commutative inspired electrical charged EEH spacetime.

The charged non-commutative inspired EEH metrics show several interesting aspects. The non-commutative terms certainly affect the horizon radius and the non-commutative corrections are relevant in connection with holographic superconductors [28]. For our models, we showed that the weak energy condition is satisfied in a region near the source depending on the values of the parameters M, Q_e, A and θ. This significant result is a natural consequence of the use of non-commutative distributions of mass and charge: these classes of spacetimes possess an inner de Sitter core at distances $r \sim 2\sqrt{\theta}$, the space–time is not globally hyperbolic, and the associated cosmological constant, with a pure non-commutative origin, is responsible for the non-singular behaviour of the solutions.

We also addressed the formation of shadows for the non-commutative inspired EEH metrics. The non-commutative shadow seems to give small corrections to the classical result; this modification may be susceptible to observation using new generation interferometers and it is relevant when probing quantum effects in gravity. It would be interesting to extend the present analysis to non-commutative inspired models where rotation is present.

Acknowledgements

AM acknowledges support from DAAD.

References

[1] M. Maggiore, A generalized uncertainty principle in quantum gravity, Phys. Lett. B 304 (1993) 65–69, https://doi.org/10.1016/0370-2693(93)91401-8, arXiv:hep-th/9301067.

[2] R. Banerjee, S. Gangopadhyay, S.K. Modak, Voros product, noncommutative Schwarzschild black hole and corrected area law, Phys. Lett. B 686 (2010) 181–187, https://doi.org/10.1016/j.physletb.2010.02.034, arXiv:0911.2123.

[3] A. Smailagic, E. Spallucci, UV divergence free QFT on noncommutative plane, J. Phys. A 36 (2003) L517–L521, https://doi.org/10.1088/0305-4470/36/39/103, arXiv:hep-th/0308193.

[4] A. Smailagic, E. Spallucci, Lorentz invariance, unitarity in UV-finite of QFT on noncommutative spacetime, J. Phys. A 37 (2004) 1–10, https://doi.org/10.1088/0305-4470/37/28/008, arXiv:hep-th/0406174.

[5] P. Nicolini, A. Smailagic, E. Spallucci, Noncommutative geometry inspired Schwarzschild black hole, Phys. Lett. B 632 (2006) 547–551, https://doi.org/10.1016/j.physletb.2005.11.004, arXiv:gr-qc/0510112.

[6] P. Nicolini, Noncommutative black holes, the final appeal to quantum gravity: a review, Int. J. Mod. Phys. A 24 (2009) 1229–1308, https://doi.org/10.1142/S0217751X09043353, arXiv:0807.1939 [hep-th].

[7] L. Modesto, P. Nicolini, Charged rotating noncommutative black holes, Phys. Rev. D 82 (2010) 104035, https://doi.org/10.1103/PhysRevD.82.104035, arXiv:1005.5605.

[8] M. Born, L. Infeld, Foundations of the new field theory, Proc. R. Soc. Lond. Ser. A 144 (1934) 425–451.

[9] W. Heisenberg, H. Euler, Folgerungen aus der Diracschen Theorie des Positrons, Z. Phys. 98 (1936) 714–732, arXiv:physics/0605038.

[10] V. Perlick, Gravitational lensing from a spacetime perspective, Living Rev. Relativ. 7 (1) (2004) 9, https://doi.org/10.12942/lrr-2004-9.
[11] A. Grenzebach, V. Perlick, C. Lämmerzahl, Photon regions and shadows of Kerr–Newman-NUT black holes with a cosmological constant, Phys. Rev. D 89 (12) (2014) 124004, https://doi.org/10.1103/PhysRevD.89.124004, arXiv:1403.5234.
[12] A. Grenzebach, Aberrational effects for shadows of black holes, in: Fund. Theor. Phys., vol. 179, 2015, pp. 823–832, arXiv:1502.02861.
[13] P.V.P. Cunha, C.A.R. Herdeiro, Shadows and strong gravitational lensing: a brief review, Gen. Relativ. Gravit. 50 (4) (2018) 42, https://doi.org/10.1007/s10714-018-2361-9, arXiv:1801.00860.
[14] D. Psaltis, Testing general relativity with the Event Horizon Telescope, arXiv:1806.09740.
[15] M. Sharif, S. Iftikhar, Shadow of a charged rotating non-commutative black hole, Eur. Phys. J. C 76 (11) (2016) 630, https://doi.org/10.1140/epjc/s10052-016-4472-3, arXiv:1611.00611.
[16] A. Saha, S.M. Modumudi, S. Gangopadhyay, Shadow of a noncommutative geometry inspired Ayón Beato García black hole, Gen. Relativ. Gravit. 50 (8) (2018) 103, https://doi.org/10.1007/s10714-018-2423-z, arXiv:1802.03276.
[17] J.M. Tejeiro, A. Larranaga, Noncommutative geometry inspired rotating black hole in three dimensions, Pramana 78 (2012) 155–164, https://doi.org/10.1007/s12043-011-0206-0, arXiv:1004.1120.
[18] J. Liang, B. Liu, Thermodynamics of noncommutative geometry inspired BTZ black hole based on Lorentzian smeared mass distribution, Europhys. Lett. 100 (2012) 30001, https://doi.org/10.1209/0295-5075/100/30001.
[19] F. Rahaman, P.K.F. Kuhfittig, B.C. Bhui, M. Rahaman, S. Ray, U.F. Mondal, BTZ black holes inspired by noncommutative geometry, Phys. Rev. D 87 (8) (2013) 084014, https://doi.org/10.1103/PhysRevD.87.084014, arXiv:1301.4217.
[20] A. González, R. Linares, M. Maceda, O. Sánchez-Santos, Noncommutative Einstein–Proca spacetime, Phys. Rev. D 90 (12) (2014) 124085, https://doi.org/10.1103/PhysRevD.90.124085.
[21] K.A. Bronnikov, Comment on 'Regular black hole in general relativity coupled to nonlinear electrodynamics', Phys. Rev. Lett. 85 (2000) 4641, https://doi.org/10.1103/PhysRevLett.85.4641.
[22] K.A. Bronnikov, Regular magnetic black holes and monopoles from nonlinear electrodynamics, Phys. Rev. D 63 (2001) 044005, https://doi.org/10.1103/PhysRevD.63.044005, arXiv:gr-qc/0006014.
[23] A. Burinskii, S.R. Hildebrandt, New type of regular black holes and particle-like solutions from NED, Phys. Rev. D 65 (2002) 104017, https://doi.org/10.1103/PhysRevD.65.104017, arXiv:hep-th/0202066.
[24] K.A. Bronnikov, Comment on "Construction of regular black holes in general relativity", Phys. Rev. D 96 (12) (2017) 128501, https://doi.org/10.1103/PhysRevD.96.128501, arXiv:1712.04342.
[25] M. Abramowitz, I.A. Stegun (Eds.), Handbook of Mathematical Functions with Formulas, Graphs, and Mathematical Tables, Dover Publications, New York, 1965.
[26] R. Ruffini, Y.-B. Wu, S.-S. Xue, Einstein–Euler–Heisenberg theory and charged black holes, Phys. Rev. D 88 (2013) 085004, https://doi.org/10.1103/PhysRevD.88.085004, arXiv:1307.4951.
[27] J.L. Synge, The escape of photons from gravitationally intense stars, Mon. Not. R. Astron. Soc. 131 (1966) 463, https://doi.org/10.1093/mnras/131.3.463.
[28] S. Pramanik, S. Ghosh, AdS-CFT correspondence in noncommutative background, related thermodynamics and holographic superconductor in magnetic field, arXiv:1509.07825.